Biochemical Pharmacology 188 (2021) 114578

Contents lists available at ScienceDirect

Biochemical Pharmacology

journal homepage: www.elsevier.com/locate/biochempharm

GLP-1 improves the neuronal supportive ability of astrocytes in Alzheimer's disease by regulating mitochondrial dysfunction via the cAMP/PKA pathway

Yunzhen Xie [a], Jiaping Zheng [b], Shiqi Li [a], Huiying Li [a], Yu Zhou [a], Wenrong Zheng [a], Meilian Zhang [c,d], Libin Liu [b], Zhou Chen [a,c,*]

[a] School of Pharmacy, Fujian Medical University, Fuzhou 350122, China
[b] Department of Endocrinology, Fujian Medical University Union Hospital, Fuzhou 350001, China
[c] Fujian Key Laboratory of Natural Medicine Pharmacology, Fujian Medical University, Fuzhou 350122, China
[d] Department of Ultrasound, Fujian Provincial Maternity and Children's Hospital, Affiliated Hospital of Fujian Medical University, Fuzhou 350001, China

ARTICLE INFO

Keywords:
Glucagon-like peptide-1
Astrocyte
Mitochondrial dysfunction
Alzheimer's disease
cAMP/PKA pathway

ABSTRACT

The glucagon-like peptide-1 (GLP-1) was shown to have neuroprotective effects in Alzheimer's disease (AD). However, the underlying mechanism remains elusive. Astrocytic mitochondrial abnormalities have been revealed to constitute important pathologies. In the present study, we investigated the role of astrocytic mitochondria in the neuroprotective effect of GLP-1 in AD. To this end, 6-month-old 5 × FAD mice were subcutaneously treated with liraglutide, a GLP-1 analogue (25 nmol/kg/qd) for 8 weeks. Liraglutide ameliorated mitochondrial dysfunction and prevented neuronal loss with activation of the cyclic adenosine 3′,5′-monophosphate (cAMP)/phosphorylate protein kinase A (PKA) pathway in the brain of 5 × FAD mice. Next, we exposed astrocytes to β-amyloid (Aβ) in vitro and treated them with GLP-1. By activating the cAMP/PKA pathway, GLP-1 increased the phosphorylation of DRP-1 at the s637 site and mitigated mitochondrial fragmentation in Aβ-treated astrocytes. GLP-1 further improved the Aβ-induced energy failure, mitochondrial reactive oxygen species (ROS) overproduction, mitochondrial membrane potential (MMP) collapse, and cell toxicity in astrocytes. Moreover, GLP-1 also promoted the neuronal supportive ability of Aβ-treated astrocytes via the cAMP/PKA pathway. This study revealed a new mechanism behind the neuroprotective effect of GLP-1 in AD.

1. Introduction

Astrocytes are the most abundant neural cells in the central nervous system (CNS) and have been shown to play vital roles in maintaining brain homeostasis, neuronal nutrient supply, the secretion of neurotrophic factors, and synaptic plasticity [1]. Accordingly, astrocytic malfunction is associated with nerve injury and neurodegeneration. Clinical and preclinical research has revealed that astrocytes participate in the pathological process of Alzheimer's disease (AD) [2–5]. Astrocytes from APP/PS1 mice were shown to cause a marked decrease in dendritic complexity in co-cultured neurons [6]. In addition, neurons co-cultured with 3 × Tg-AD mouse astrocytes were characterized by more apoptotic nuclei and fewer viable cells [7]. However, there are still many unknowns about the role of astrocytes in AD.

Mitochondria are known to be critical organelles of cells and govern various physiological processes, such as energy metabolism, antioxidant production, cell survival, and death in astrocytes [8]. Accumulating evidence has indicated that astrocytic mitochondrial abnormalities might be involved in the pathogenesis of CNS diseases [9–12]. Regarding AD, a global metabolomic profiling demonstrated that primary astrocyte generated from 5 × FAD transgenic mice exhibited alterations in the tricarboxylic acid cycle, and similar metabolic changes could be induced by exogenous β-amyloid (Aβ) peptide [13]. Furthermore, immortalized hippocampal astrocytes from 3 × Tg-AD mice

Abbreviations: AD, Alzheimer's disease; Aβ, β-amyloid; ATP, adenosine triphosphate; BDNF, brain-derived neurotrophic factor; cAMP, cyclic adenosine 3′,5′-monophosphate; CNS, central nervous system; DRP1, dynamin-related protein 1; GLP-1, glucagon-like peptide-1; MFN2, mitofusin 2; MMP, mitochondrial membrane potential; OCR, oxygen consumption rate; OPA1, optic atrophy 1; PKA, phosphorylate protein kinase A; ROS, reactive oxygen species.

* Corresponding author at: School of Pharmacy, Fujian Medical University, Fuzhou 350122, China.
E-mail address: chenzhou@fjmu.edu.cn (Z. Chen).

https://doi.org/10.1016/j.bcp.2021.114578
Received 24 January 2021; Received in revised form 17 April 2021; Accepted 19 April 2021
Available online 22 April 2021

showed impaired mitochondrial energy metabolism and increased reactive oxygen species (ROS) production [14].

The glucagon-like peptide-1 (GLP-1) is a 30-amino-acid incretin hormone known to act as a neuropeptide in the brain, and has been shown to have neurotrophic and neuroprotective effects in the CNS [15]. Native GLP-1 is rapidly metabolized and inactivated by dipeptidyl peptidase-4 (DPP-4) and subsequently eliminated by renal. Thus, GLP-1 analogues with structural modification are often applied to in vivo therapy [16]. It is reported that GLP-1 exerts its effects by binding to and activating GLP-1 receptor (GLP-1R) [16], which could be reversed by GLP-1R antagonist or knockout [17,18]. GLP-1Rs are widely distributed in brain areas closely related to memory and learning [19,20]. Activation of the GLP-1R could elevate the intracellular cyclic adenosine 3′,5′-monophosphate (cAMP) signaling pathway level by stimulating adenylate cyclase and phosphorylating protein kinase A (PKA), ultimately increasing the release of neurotransmitters and promoting excitatory synaptic transmission [21,22]. Moreover, GLP-1, as well as its analogues and receptor agonists, have been shown to prevent neurodegeneration in experimental AD models [23–25]. Our previous studies reported that GLP-1 analogue could rescue cognitive impairment in AD mice, and the mechanism behind this was associated with mitochondrial dynamics [26,27]. However, the specifics of the underlying mechanism remain to be further explored.

In the present study, we explored the mechanism of GLP-1 in alleviating neuronal damage in AD. We found that by activating the cAMP/PKA pathway, GLP-1 mitigated mitochondrial overfission, and simultaneously improved mitochondrial functions in Aβ-treated astrocytes, thus enhancing its neuronal supportive ability.

2. Materials and methods

2.1. Reagents

Liraglutide (Victoza®) was purchased from Novo Nordisk (Bagsværd, Denmark). $A\beta_{1\text{-}42}$ was purchased from ChinaPeptides (Shanghai, China). GLP-1 was purchased from MedChemExpress (Monmouth Junction, NJ, USA). L-glutamine, 1,1,1,3,3,3-hexafluoro-2-propanol (HFIP), and H-89 were purchased from Sigma-Aldrich (St. Louis, MO, USA). D-Hank's solution and Dulbecco's modified Eagle's medium (DMEM)/F12 were purchased from Hyclone (Logan, UT, USA). Fetal bovine serum (FBS), penicillin/streptomycin, Neurobasal medium, and B27 were purchased from Gibco (Carlsbad, CA, USA). For the mitochondrial stress test, Seahorse XF DMEM, glutamine, glucose, pyruvate, oligomycin, carbonyl cyanide 4-(trifluoromethoxy)phenylhydrazone (FCCP), rotenone & antimycin A were purchased from Agilent Technologies (Santa Clara, CA, USA).

2.2. Animals and drug administration

Transgenic 5 × FAD mice were obtained from The Jackson Laboratory and the generation of 5 × FAD mice has been described in previous study [28]. 6-month-old 5 × FAD mice were randomly assigned to AD group and AD + Lira group, whereas nontransgenic wild-type littermates were used as control (WT group) (n = 10 mice per group). All mice were housed in a specific pathogen-free environment with a 12 h light/dark cycle under standard laboratory conditions at a temperature of 20 ± 3 °C and humidity of 40–60%. Mice in the AD + Lira group were subcutaneously administered 25 nmol/kg/qd liraglutide for 8 weeks [26], whereas mice in the WT and AD groups received an equal amount of 0.9% saline according to the same regimen.

All animal protocols were conducted in accordance with the National Institutes of Health Guide for the Care and Use of Laboratory Animals (NIH eighth edition, revised 2011) and Institutional Animal Care and Use Committee of Fujian Medical University (No. FJMU IACUC 2018-035).

2.3. Tissue preparation

After 8 weeks of liraglutide administration, mice were anesthetized with an intraperitoneal injection of 60 mg/kg pentobarbital sodium [29]. For Nissl staining, mice were transcardially perfused with 0.9% saline followed by 4% paraformaldehyde. Brain tissues were dissected and fixed in 4% paraformaldehyde in PBS. Then, brain tissues were embedded in paraffin and cut into 4-μm-thick paraffin sections. For western blot and enzyme-linked immunosorbent assays (ELISA), brain tissues were dissected on ice and then stored at −80 °C.

2.4. Nissl staining

Paraffin sections were stained with Nissl staining solution (Sevicebio, Wuhan, China) for 10 min and then dehydrated for observation. Sections were scanned by Panoramic DESK (3DHISTECH, Hungary) and the microphotographs were generated by Panoramic Scanner (3DHISTECH). Representative images of the cortex and hippocampus were acquired using the CaseViewer software (3DHISTECH). The number of cells in the cortex and hippocampus was counted using the Fiji-Image J software (National Institutes of Health, USA).

2.5. Primary cell cultures

Cultures of primary astrocytes and neurons were prepared from P0-P1 Sprague-Dawley rat pups. Cortices were dissected and pooled into D-Hank's solution, and the meninges were carefully removed. For astrocyte cultures, cortices were digested in 0.25% trypsin (Gibco, Carlsbad, CA, USA) for 15 min at 37 °C, and the resulting cell suspensions were seeded in 25 cm^2 culture flasks. Cells were cultured in DMEM/F12 supplemented with 10% FBS, 1% penicillin/streptomycin, and 2 mM L-glutamine at 37 °C and 5% CO_2. The astrocyte culture medium was changed every 3 days. After 10–14 days, cultures were shaken in an orbital shaker at 37 °C at a speed of 200 rpm for 18 h. The purity of astrocytes was identified using anti-glial fibrillary acidic protein (GFAP) immunofluorescence staining. Astrocytes from passage 3 were used for subsequent experiments. For neuron cultures, cortices were digested in papain dissociation solution (Worthington, Lakewood, NJ, USA) for 20 min at 37 °C. The resulting cell suspensions were plated on poly-D-lysine-coated cover glass in 6-well plates at a density of 5×10^4 cells/mL. Neurons were cultured in Neurobasal medium supplemented with 2% B27, 1% penicillin/streptomycin, and 0.5 mM L-glutamine. Neurons at days in vitro (DIV) 3 were used for coculturing with astrocytes.

Astrocyte-neuron co-culture system was established according to a previously described method [30]. Briefly, astrocytes were plated on poly-D-lysine-coated polycarbonate membranes of Transwell inserts (0.4 μm, Corning, Corning, NY, USA) at a density of 8×10^4 cells/mL. After 48 h, the astrocyte culture medium was replaced with neuron culture medium and cells were cultured for a further 24 h. Subsequently, the astrocytes were treated with drugs before Transwell inserts being transferred to the top side of 6-well plates and co-cultured with neurons. The co-culture system was maintained until neurons reached DIV 10.

2.6. $A\beta_{1\text{-}42}$ preparation

$A\beta_{1\text{-}42}$ peptides were dissolved in hexafluoroisopropanol (HFIP) and lyophilized. Soluble oligomeric $A\beta_{1\text{-}42}$ was prepared by dissolving $A\beta_{1\text{-}42}$ peptides in dimethyl sulfoxide (DMSO) and then diluting the mixture in PBS to a final concentration of 400 μM. Obtained solutions were incubated overnight at 4 °C and stored at −20 °C.

2.7. Elisa

To measure cortex cAMP contents, brain tissues were homogenized with PBS. To measure intracellular cAMP levels, cells were lysed using RIPA buffer (Beyotime, Shanghai, China). To detect the secretion of

brain-derived neurotrophic factor (BDNF) from astrocytes, the cell culture supernatant was collected. All specimens mentioned above were centrifuged at 3000 rpm for 20 min, and the supernatants were collected for experiments. The mouse cAMP ELISA kit, rat cAMP ELISA kit, and rat BDNF ELISA kit were performed according to the manufacturer's instructions (Shanghai Enzyme-linked Biotechnology, Shanghai, China).

2.8. Measurement of ATP

The production of ATP in brain tissues and cells was measured using an Enhanced ATP assay kit (Beyotime) according to the manufacturer's instructions. Tissue or cell lysate was centrifuged for 5 min at 12 000 *g* and 4 °C, and then 20 μL supernatant and 100 μL ATP detection working solution were added to a 96-well opaque plate. Luminescence was detected using a SpectraMax iD3 microplate reader (Molecular Devices, San Jose, CA, USA) and the concentration of ATP was calculated according to a standard curve.

2.9. ROS production

The production of ROS in brain tissues was measured using ROS (DCFH-DA) assay kit (Quanzhou Ruixin Biotechnolgy, Quanzhou, China) according to the manufacturer's instructions. Briefly, tissues were homogenized with PBS and disrupted by ultrasonication. Then the samples were centrifuged for 15 min at 3000 rpm and the supernatants were collected. The supernatants were incubated with DCFH-DA probe for 30 min at 37 °C, and detected at excitation and emission wavelengths of 488 and 525 nm using a microplate reader (Molecular Devices).

2.10. Western blot analysis

Tissues or cells were lysed using RIPA buffer containing protease and phosphatase inhibitors (Boster, Wuhan, China). Protein concentrations were quantified using a BCA assay kit (Boster) according to the manufacturer's instructions. Equal amounts of protein from cells were electrophoresed on 10–12% sodium dodecyl sulfate–polyacrylamide (SDS-PAGE) gels (Boster) and electrotransferred onto polyvinylidene difluoride (PVDF) membranes activated by methanol. Membranes were blocked with 5% dried skimmed milk in TBST for 2 h and then incubated with primary antibodies at 4 °C overnight. Primary antibodies used were as follows: p-DRP1(s637) (1:1000, #4867, Cell Signaling, Danvers, MA, USA), t-DRP1 (1:1000, #8570, Cell Signaling), MFN2 (1:1000, #ab56889, Abcam, Cambridge, MA, USA), OPA1 (1:1000, ab157457, Abcam), and GAPDH (1:1000, #5174, Cell Signaling). After incubation with primary antibodies, membranes were washed in TBST and incubated with horseradish peroxidase (HRP)-conjugated anti-rabbit or anti-mouse secondary antibodies (1:1000, #7074 or #7076, Cell Signaling) for 2 h at 25 °C. Then, bands were detected using ECL (SAB, MD, USA) and visualized using a ChemiDoc™ Imaging System (BioRad, Danvers, MA, USA). Blot images were analyzed using the Image J software and protein expression levels were normalized to GAPDH levels.

2.11. Mitochondrial morphology analysis

Mitochondrial morphology was determined using MitoTracker Red staining (Beyotime). Mitochondria were labeled with 50 nM MitoTracker Red probe for 30 min at 37 °C. Representative images of mitochondrial morphology were acquired using a Leica SP5 confocal microscope (Leica, Wetzlar, Germany). Quantitative analysis of mitochondrial morphology was performed using the Image J software, and the following parameters were collected: major axis, minor axis, perimeter, and area. The aspect ratio (AR = major axis/minor axis) and form factor (FF = perimeter^2/4π × area) represent the length and degree of branching of mitochondria.

2.12. Mitochondrial ROS production

Mitochondria in astrocytes were labeled with 100 nM MitoTracker Green probe (Beyotime) for 20 min at 37 °C. Astrocytes were then loaded with 5 μM MitoSOX Red indicator (Invitrogen, Carlsbad, CA, USA) for 10 min at 37 °C to measure mitochondrial ROS production. Nuclei were stained with Hoechst 33432 (Beyotime) for 10 min at 37 °C. Representative images were acquired using a Leica SP5 confocal microscope and red fluorescence intensity was determined using the Image J software.

2.13. Measurement of cellular oxygen consumption rate (OCR)

Astrocytes were plated at a density of 8×10^3 cells per well in XFe24 V7 cell culture microplate (Agilent Technologies, Santa Clara, CA, USA) and treated with drugs before cells reached 80–90% confluency. Before measurement, astrocytes culture medium was replaced with Seahorse XF DMEM supplemented with 2 mM glutamine, 10 mM glucose, and 1 mM pyruvate (pH = 7.4). For the mitochondrial stress test, the oxygen consumption rate (OCR) of primary astrocytes was determined using Seahorse XFe24 Flux Analyzer (Agilent Technologies) following subsequent injections of 1 μM oligomycin, 2 μM FCCP, and 0.5 μM rotenone&antimycin A at final concentration. Data were analyzed using the Seahorse Wave Desktop software (Agilent Technologies).

2.14. Measurement of mitochondrial membrane potential (MMP)

The mitochondrial membrane potential was determined using the JC-1 mitochondrial membrane potential assay kit (Beyotime) according to the manufacturer's instructions. Astrocytes were incubated with JC-1 staining working solution for 20 min at 37 °C and washed 3 times with JC-1 staining wash buffer. Representative images were acquired using a Leica SP5 confocal microscope, and fluorescence intensity was determined using the Image J software. As is known, JC-1 forms aggregates in the mitochondrial matrix at high MMP, emitting red fluorescence. When MMP collapses, JC-1 remains in the monomeric form, emitting green fluorescence. Consequently, MMP was expressed by a decrease in the ratio of red/green fluorescence intensity.

2.15. Cell viability assay

The viability of the astrocytes was assessed using the MTT (Sigma-Aldrich, St. Louis, MO, USA) according to the manufacturer's instructions. Briefly, 8–10 × 10^3 cells/per well were seeded onto a 96-well plate. After treatment with drugs, 10 μL MTT solution (1 mg/mL) per 100 μL DMEM/F12 was added to each well and cells were incubated for 4 h. After 4 h, the medium was removed and 150 μL DMSO was added into each well to resolve the MTT formazan crystals. The absorbance at 490 nm was measured using a microplate spectrophotometer (BioTek, Winooski, VT, USA).

2.16. Immunofluorescence

Neurons were fixed in 4% paraformaldehyde for 15 min, then permeabilized and blocked in 0.3% Triton X-100 and 5% bovine serum albumin for 1 h at 37 °C. Subsequently, neurons were first incubated with anti-βIII-tubulin primary antibody (1:400, ab78078, Abcam) overnight at 4 °C and then with Alexa 488 secondary antibody (1:400, ab150113, Cell Signaling) for 2 h at 37 °C. Representative images were acquired using a Leica SP5 confocal microscope. The neuronal morphology was analyzed using the Image J software and parameters, such as axon length, number of neurites from the soma, number of secondary branches, and total neurite length were acquired. Sholl analysis was performed according to the previous study [31].

2.17. Hoechst and propidium iodide (PI) staining

Neurons were sequentially incubated with Hoechst (Beyotime) and PI (Beyotime) staining solutions for 20 min at 4 °C. Representative images were acquired using a fluorescent microscope (Olympus, Tokyo, Japan).

2.18. Statistic analysis

All data were presented as the mean ± standard error of the mean (SEM). Statistical analyses were performed using one-way or two-way ANOVA with Bonferroni's post-hoc test using SPSS Statistics 21.0 (IBM, Armonk, NY, USA) and GraphPad Prism 7.0 (GraphPad Software, La Jolla, CA, USA). Statistical significance was set at $P < 0.05$.

3. Results

3.1. Liraglutide ameliorated mitochondrial dysfunction, prevented neuron loss, and activated the cAMP/PKA pathway in the brain of 5 × FAD mice

Our previous study demonstrated that exenatide, a GLP-1 analogue, could improve cognition and regulate mitochondrial dynamics in the brain of 5 × FAD mice [27]. However, the underlying mechanism remained elusive.

The cAMP/PKA pathway is deeply involved in the regulation of mitochondrial dynamics. To further explore the role of the cAMP/PKA pathway in the neuroprotective effect of GLP-1 against AD, we treated 6-month-old 5 × FAD mice with subcutaneous injection of liraglutide, another GLP-1 analogue, for 8 weeks and evaluated the cortex cAMP contents and PKA protein expression levels. Compared with wild-type mice, we observed that 5 × FAD mice showed a reduction in cAMP level ($P < 0.01$, Fig. 1A) and were also characterized by inhibition of phosphorylation of PKA ($P < 0.01$, Fig. 1B-C). In contrast, we found that

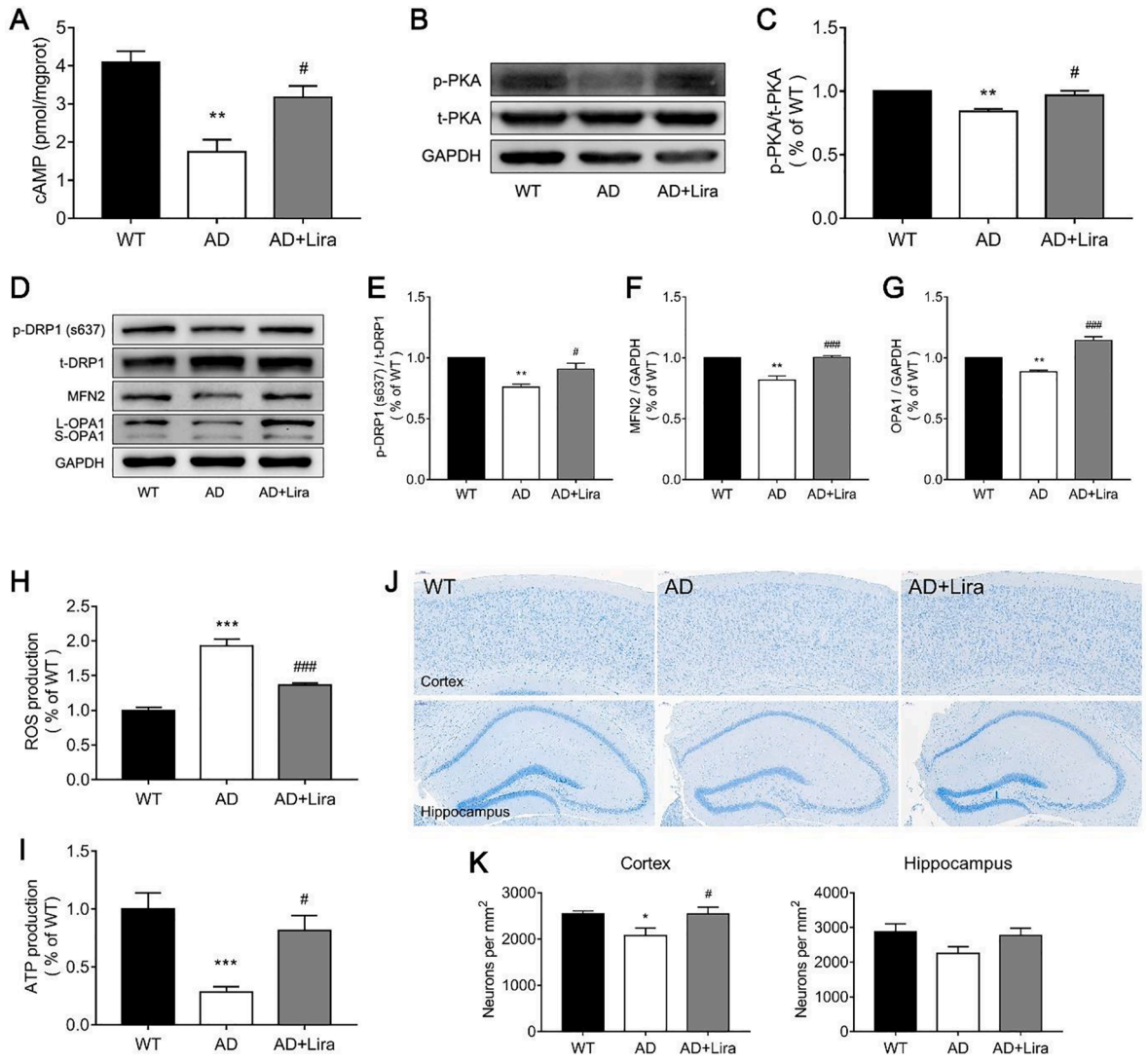

Fig. 1. Liraglutide ameliorated mitochondrialdysfunction, prevented neuron loss, and activated cAMP/PKA pathway in the brain of 5 × FAD mice. (A) Cortex cAMP contents determined by ELISA. n = 5 mice/group. (B) Protein expression of cortex p-PKA determined by western blot analysis. (C) Relative quantitative analysis of cortex p-PKA protein expression. n = 3 mice/group. (D) Cortex protein expression of mitochondrial dynamics related proteins determined by western blot analysis. (E-G) Relative quantitative analysis of cortex p-DRP1 (s637) (E), MFN2 (F) and OPA1 (G) protein expression. n = 3 mice/group. (H) ROS production determined by ELISA. n = 5 mice/group. (I) ATP production. n = 5 mice/group. (J) Representative images of the Nissl-stained positive neurons in cortex and hippocampus. Scale bar = 100 μm. (K) Quantitative analysis of the number of Nissl-stained positive neurons per mm^2. n = 3 mice/group. $^{**}P < 0.01$, $^{***}P < 0.001$ vs. WT; $\#P < 0.05$, $\#\#\#P < 0.001$ vs. AD.

liraglutide significantly increased the cAMP level ($P < 0.05$, Fig. 1A) and p-PKA protein expression level ($P < 0.05$, Fig. 1B-C) in AD + Lira group.

Consistent with our previous study [27], our results showed that liraglutide reversed the decrease of phosphorylation of dynamin-related protein 1 (p-DRP1) at the s637 site, mitofusin 2 (MFN2), and optic atrophy 1 (OPA1) expression levels ($P < 0.05$, $P < 0.001$, $P < 0.001$, respectively, Fig. 1D-G), rescued the overproduction of ROS ($P < 0.05$, Fig. 1H), and enhanced the production of ATP ($P < 0.05$, Fig. 1I) in 5 × FAD mice.

In addition, we also found that liraglutide prevented neuron loss in the brain of 5 × FAD mice. Our results from Nissl staining revealed that the number of neurons was reduced in both the cortex ($P < 0.05$, Fig. 1J-K) and hippocampus of 5 × FAD mice. Moreover, liraglutide significantly increased the number of neurons in the cortex of mice in AD + Lira group ($P < 0.05$, Fig. 1J-K).

3.2. GLP-1 prevented mitochondrial fragmentation, ameliorated mitochondrial dysfunction, and promoted cell survival in Aβ-treated astrocytes via the cAMP/PKA pathway

Astrocytic mitochondrial abnormalities have been revealed to constitute important pathologies in AD. To investigate the effects of GLP-1 on astrocytes, we generated an in vitro AD model based on astrocytes and treated the cells with GLP-1. Primary astrocyte cultures were pretreated with 100 nM GLP-1 for 2 h [32] and then incubated with 10 μM $A\beta_{1\text{-}42}$ for 24 h [33]. Furthermore, PKA inhibitor H-89 was applied to validate the role of the cAMP/PKA pathway in the regulative effect of GLP-1 (as cAMP is known to mainly work by activating PKA [34]). Astrocytes in Aβ + GLP-1 + H-89 group were treated with 10 μM H-89 [35] combined with 100 nM GLP-1 for 2 h before being exposed to 10 μM $A\beta_{1\text{-}42}$.

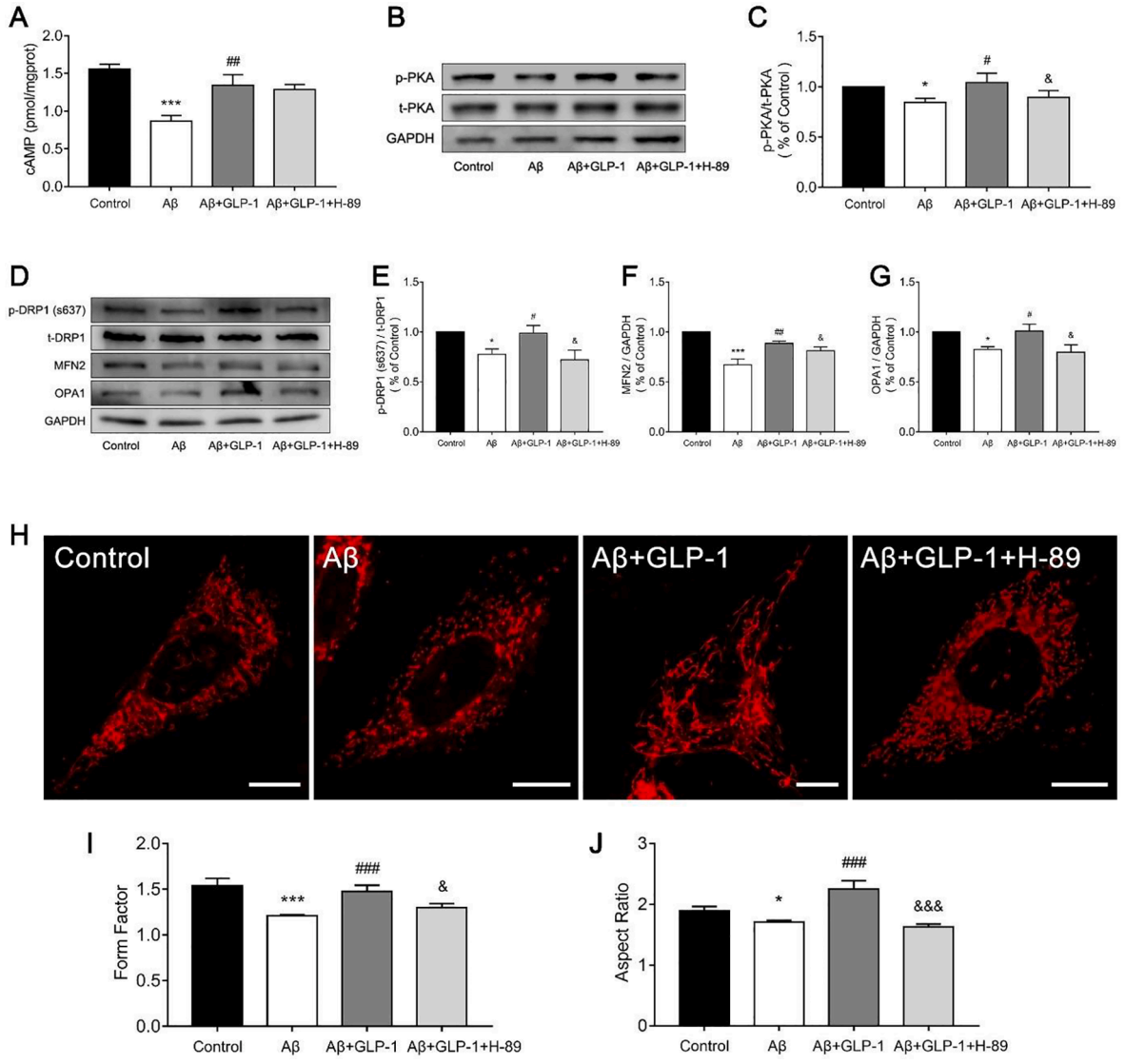

Fig. 2. GLP-1 prevented mitochondrial fragmentation in Aβ-treated astrocytes via the cAMP/PKA pathway. Primary astrocyte cultures were pre-treated with 100 nM GLP-1 for 2 h and then incubated with 10 μM $A\beta_{1\text{-}42}$ for 24 h. Astrocytes in Aβ + GLP-1 + H-89 group were treated with 10 μM H-89 co-incubated with GLP-1. (A) Intracellular cAMP levels determined by ELISA. n = 5 wells/group. (B) Protein expression of p-PKA determined by western blot analysis. (C) Relative quantitative analysis of p-PKA protein expression. n = 3 wells/group. (D) Protein expression of mitochondrial dynamics related proteins determined by western blot analysis. (E-G) Relative quantitative analysis of p-DRP1 (s637) (E), MFN2 (F), and OPA1 (G) protein. n = 3 wells/group. (H) Mitochondrial morphology was revealed through MitoTracker Red staining and analyzed using the Image J software. Scale bar = 10 μm. (I-J) Quantitative analysis of mitochondrial morphology. Morphological analysis of mitochondria. Form factor (FF) (I) and aspect ratio (AR) (J) were determined using the Image J software. n = 3 wells/group. *$P < 0.05$, ***$P < 0.001$ vs. Control; #$P < 0.05$, ##$P < 0.01$ vs. Aβ; &$P < 0.05$ vs. Aβ + GLP-1. (For interpretation of the references to colour in this figure legend, the reader is referred to the web version of this article.)

3.2.1. GLP-1 activated cAMP/PKA pathway in Aβ-treated astrocytes

We observed that exposure of astrocytes to 10 μM Aβ for 24 h caused decreases in intracellular cAMP level ($P < 0.001$, Fig. 2A) and p-PKA protein expression ($P < 0.001$, Fig. 2B-C), whereas GLP-1 elevated cAMP levels ($P < 0.01$, Fig. 2A) and promoted the phosphorylation of PKA ($P < 0.05$, Fig. 2B-C) in Aβ-treated astrocytes, consistent with our in vivo findings. And the phosphorylation of PKA was inhibited by 10 μM H-89 ($P < 0.05$, Fig. 2B-C), whereas the levels of cAMP remained unchanged.

3.2.2. GLP-1 prevented mitochondrial fragmentation in Aβ-treated astrocytes via the cAMP/PKA pathway

The balance between mitochondrial fission and fusion, which is regulated by GTPase-dependent proteins, such as DRP1, MFN2, and OPA1, contributes to the normal function of mitochondria [36]. Our immunoblot analysis results showed that Aβ induced a significant decrease of p-DRP1 (s637), MFN2 and OPA1 expression ($P < 0.05$, $P < 0.001$ and $P < 0.05$, respectively; Fig. 2D-G), whereas GLP-1 significantly restored the Aβ-induced downregulation of these proteins in astrocytes ($P < 0.05$ for all, Fig. 2D-G). We further determined the mitochondrial morphology in astrocytes using the MitoTracker Red staining, and quantified the values of the mitochondrial form factor (FF) and aspect ratio (AR) [37]. As shown in Fig. 2H, mitochondria in the control group displayed an elongated tubular structure and were equally distributed throughout the cytoplasm. In contrast, Aβ induced a redistribution in the mitochondrial size to smaller and rounder mitochondria accompanied with reduced FF ($P < 0.001$, Fig. 2I) and AR values ($P <$

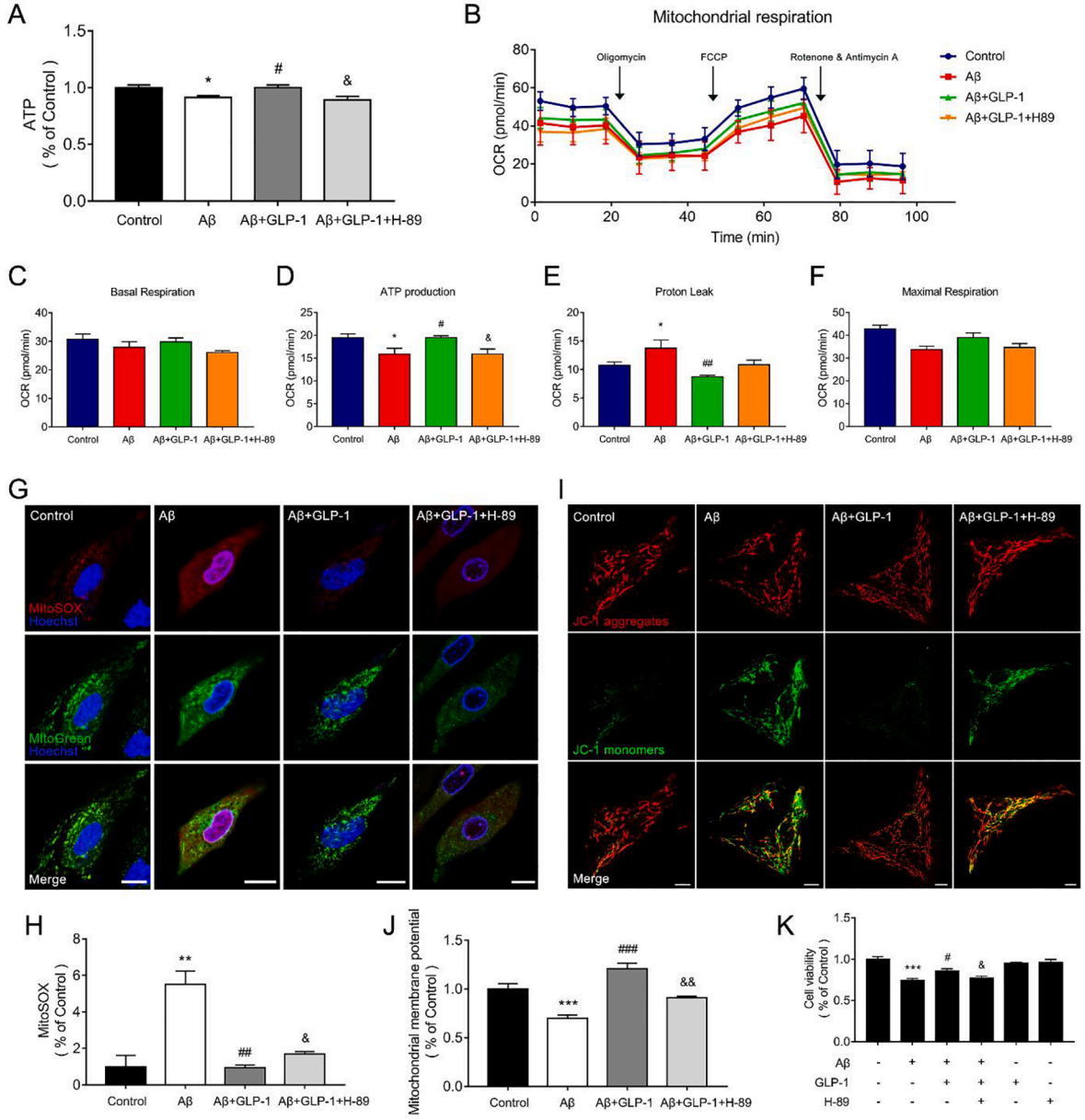

Fig. 3. GLP-1 ameliorated mitochondrial dysfunction and promoted cell survival in Aβ-treated astrocytes via the cAMP/PKA pathway. (A) ATP production. (B) Profiles of oxygen consumption rates (OCR). (C-F) Basal respiration (C), ATP production (D), proton leak (E), and maximal respiration (F) were determined based on OCR. n = 5 wells/group. (G) Mitochondrial ROS production was labeled by MitoSOX staining (red), with mitochondria being labeled using MitoTracker Green staining (green). Nuclei were stained with Hoechst 33342 (blue). Scale bar = 10 μm. (H) Mitochondrial ROS production expressed by red fluorescence intensity. n = 3 wells/group. (I) Mitochondrial membrane potential (MMP) determined by JC-1 staining. JC-1 aggregates emit red fluorescence, whereas JC-1 monomers emit green fluorescence. Scale bar = 10 μm. (J) Mitochondrial membrane potential expressed by the ration of red/green fluorescence intensity. n = 3 wells/group. (K) Cell viability determined using the MTT assay. n = 5 wells/group. $^{*}P < 0.05$, $^{**}P < 0.01$, $^{***}P < 0.001$ vs. Control; $\#P < 0.05$, $\#\#P < 0.01$, $\#\#\#P < 0.001$ vs. Aβ; $\&P < 0.05$, $\&\&P < 0.01$ vs. Aβ + GLP-1. (For interpretation of the references to colour in this figure legend, the reader is referred to the web version of this article.)

0.05, Fig. 2J). In contrast, GLP-1 enabled the mitochondria of Aβ-treated astrocytes to recover to long tubular mitochondrial networks, with higher values of FF ($P < 0.001$, Fig. 2I) and AR ($P < 0.001$, Fig. 2J).

However, we also showed that the effect of GLP-1 on promoting phosphorylation of DRP1 at s637 was aborted after the inhibition of PKA ($P < 0.05$, Fig. 2D-E). And the fusion-related proteins MFN2 and OPA1 were also decreased in Aβ + GLP-1 + H-89 group ($P < 0.01$ and $P < 0.05$, respectively; Fig. 2D and F-G). Furthermore, H-89 reversed the effects of GLP-1 on mitochondrial morphology. In particular, we observed that mitochondria formed shorter tubules and showed less extensive networks accompanied by decreased FF and AR values compared with Aβ + GLP-1 group ($P < 0.05$ and $P < 0.001$, respectively, Fig. 2H–J).

3.2.3. GLP-1 ameliorated mitochondrial dysfunction and promoted cell viability in Aβ-treated astrocytes via the cAMP/PKA pathway

Mitochondria are the important energy suppliers of astrocytes through the generation of ATP. We found that Aβ induced a significant decrease of ATP production in astrocytes ($P < 0.05$, Fig. 3A), which was restored by GLP-1 ($P < 0.05$, Fig. 3A). To further assess the mitochondrial function and metabolic changes, we utilized the Seahorse XFe24 Flux Analyzer to determine mitochondrial stress by directly measuring the oxygen consumption rate (OCR). We first detected the basal respiration, showing the energetic demand of astrocytes under baseline conditions. A subsequent injection of oligomycin inhibited mitochondrial ATP synthase, thus allowing the quantification of mitochondrial ATP production to be quantified. Besides, the proton leak could serve as a sign of mitochondrial impairment. In addition, FCCP is known to uncouple oxidative phosphorylation from ATP synthesis and increase oxygen consumption to a maximal value. As such, we identified that under baseline conditions, the basal respirations were not different among Control, Aβ, and Aβ + GLP-1 groups (Fig. 3C). After oligomycin injection, Aβ group showed a reduction of mitochondrial ATP production ($P < 0.05$, Fig. 3D) and an increase in proton leak ($P < 0.05$, Fig. 3E), whereas GLP-1 increased mitochondrial ATP production ($P < 0.05$, Fig. 3D) and proton leak in Aβ + GLP-1 group ($P < 0.01$, Fig. 3E). In addition, we observed that the maximal respiration showed a trending decline in Aβ-treated astrocytes, whereas GLP-1 could restore maximal respiration to some extent, despite the lack of significant differences observed between groups (Fig. 3F).

Mitochondria are the main sites of ROS production, and hence oxidative stress caused by excessive ROS production might contribute to the collapse of MMP, resulting in cellular injury [38]. Our results showed that Aβ notably increased the generation of mitochondrial ROS in astrocytes ($P < 0.01$, Fig. 3G-H), whereas GLP-1 decreased mitochondrial ROS overproduction ($P < 0.01$, Fig. 3G-H). It should be mentioned that we determined MMP using JC-1 staining. Our results revealed that Aβ triggered the loss of MMP, as shown by a decrease in the ratio of red/green fluorescence intensity ($P < 0.001$, Fig. 3I-J), whereas MMP in Aβ + GLP-1 group was significantly higher than that in Aβ group ($P < 0.001$, Fig. 3I-J). We next evaluated the cell viability using MTT analysis. Our results showed that exposure to Aβ impaired cell viability of astrocytes ($P < 0.001$, Fig. 3K). GLP-1 did not result in significant cell toxicity to control astrocytes, but enhanced cell viability in Aβ-treated astrocytes ($P < 0.05$, Fig. 3K).

However, PKA inhibitor H-89 reversed the protective effect of GLP-1 on mitochondrial function in Aβ-treated astrocytes. More specifically, H-89 reduced ATP production ($P < 0.05$, Fig. 3A), and concomitantly decrease the mitochondrial ATP production ($P < 0.05$, Fig. 3D) and increase proton leak in Aβ + GLP-1 + H-89 group. Furthermore, H-89 resulted in an elevation in the mitochondrial ROS levels ($P < 0.05$, Fig. 3G-H) and subsequently led to the loss of MMP as expressed by a decreased ratio in the red/green fluorescence intensity ($P < 0.05$, Fig. 3I-J) in Aβ + GLP-1 + H-89 group. In addition, H-89 decreased cell viability of astrocytes in Aβ + GLP-1 + H-89 group ($P < 0.05$, Fig. 3K).

3.3. GLP-1 improved the neuronal supportive ability of Aβ-treated astrocytes via the cAMP/PKA pathway

Astrocytes are important neuronal supportive cells in the CNS that release multiple neuroprotective factors essential for neuronal development [1]. Thus, we set up an astrocyte-neuron co-culture system to evaluate the effect of GLP-1 on the neuronal supportive ability of astrocytes under exposure to Aβ.

We found that Aβ induced reductions in the secretion of BDNF from astrocytes ($P < 0.01$ for both, Fig. 4A), whereas GLP-1 restored the secretion of BDNF from Aβ-treated astrocytes ($P < 0.05$ and $P < 0.01$, respectively; Fig. 4). However, PKA inhibitor H-89 reversed the effect of GLP-1 on promoting the secretion of BDNF in Aβ + GLP-1 + H-89 group ($P < 0.05$ for both, Fig. 4A).

We next analyzed the neuronal complexity of co-cultured neurons. As shown in Fig. 4B-G, Aβ-treated astrocytes impaired the neuronal complexity of co-cultured neurons, as shown by decreased number of neurite interaction, axon length, number of neurites from soma, number of secondary branch and total neurite length ($P < 0.01$, $P < 0.001$, $P < 0.01$, $P < 0.01$, and $P < 0.01$, respectively, Fig. 4B-G). As expected, we found that GLP-1 significantly increased the number of neurite interaction, axon length, number of neurites from soma, number of secondary branch and total neurite length of neurons co-cultured with Aβ-treated astrocytes ($P < 0.001$, $P < 0.01$, $P < 0.01$, $P < 0.05$, and $P < 0.05$, respectively; Fig. 4B-G). However, H-89 significantly impaired the GLP-1-rescued neuronal complexity in Aβ-treated astrocytes ($P < 0.05$, Fig. 4B-G).

We then determined the cell death of co-cultured neurons using Hoechst/PI staining. We observed that astrocytes induced more dead co-cultured neurons in Aβ group than in control group ($P < 0.01$, Fig. 4H-I), whereas GLP-1 improved the supportive ability of Aβ-treated astrocytes, promoting the cell survival of co-cultured neurons ($P < 0.01$, Fig. 4H-I). However, inhibition of PKA reversed the protective effect of GLP-1, with astrocytes in Aβ + GLP-1 + H-89 group aggravating the cell death of co-cultured neurons ($P < 0.05$, Fig. 4H-I).

4. Discussion

This study demonstrated that GLP-1 alleviated energy deficits and prevented neuron loss in the brain of 5 × FAD mice. By activating the cAMP/PKA pathway, GLP-1 attenuated Aβ-induced astrocytic mitochondrial fragmentation, energy stress, and cell toxicity, and increased the secretion of BDNF from astrocytes, thus improving the neuronal growth and survival of co-cultured neurons.

Mitochondria are morphologically dynamic organelles that constantly undergo fusion and fission. Fission and fusion processes are known to determine the morphology and structure of the mitochondrial network, which is of paramount importance for mitochondrial homeostasis and cell survival [39,40]. Excessive mitochondrial fission has been reported to be accompanied by a decline in function, leading to neurodegeneration in AD [41]. We observed that 5 × FAD mice showed imbalanced mitochondrial dynamics in their brains accompanied by ROS overproduction and ATP reduction, as previously reported [27]. It is reported that Aβ, which is produced locally by APP processing in mitochondria, could interact with mitochondrial proteins and initiate the AD pathology by inducing mitochondrial dysfunction [42,43]. Astrocytic mitochondrial abnormalities have been revealed to constitute important pathologies in AD. Previous studies have reported that exposure of astrocytes to Aβ induced impairments in mitochondrial morphology, dynamics, and function [44–46]. GLP-1 is shown to reduce Aβ formation and accumulation [47–49], thus it is likely to improve Aβ-induced mitochondrial dysfunction. In accordance with these findings, we observed that Aβ led to mitochondrial over-fission and fragmentation, whereas GLP-1 regulated mitochondrial dynamics related proteins and reconstructed mitochondrial networks in Aβ-treated astrocytes. The balance between mitochondrial fission and fusion maintain the structure

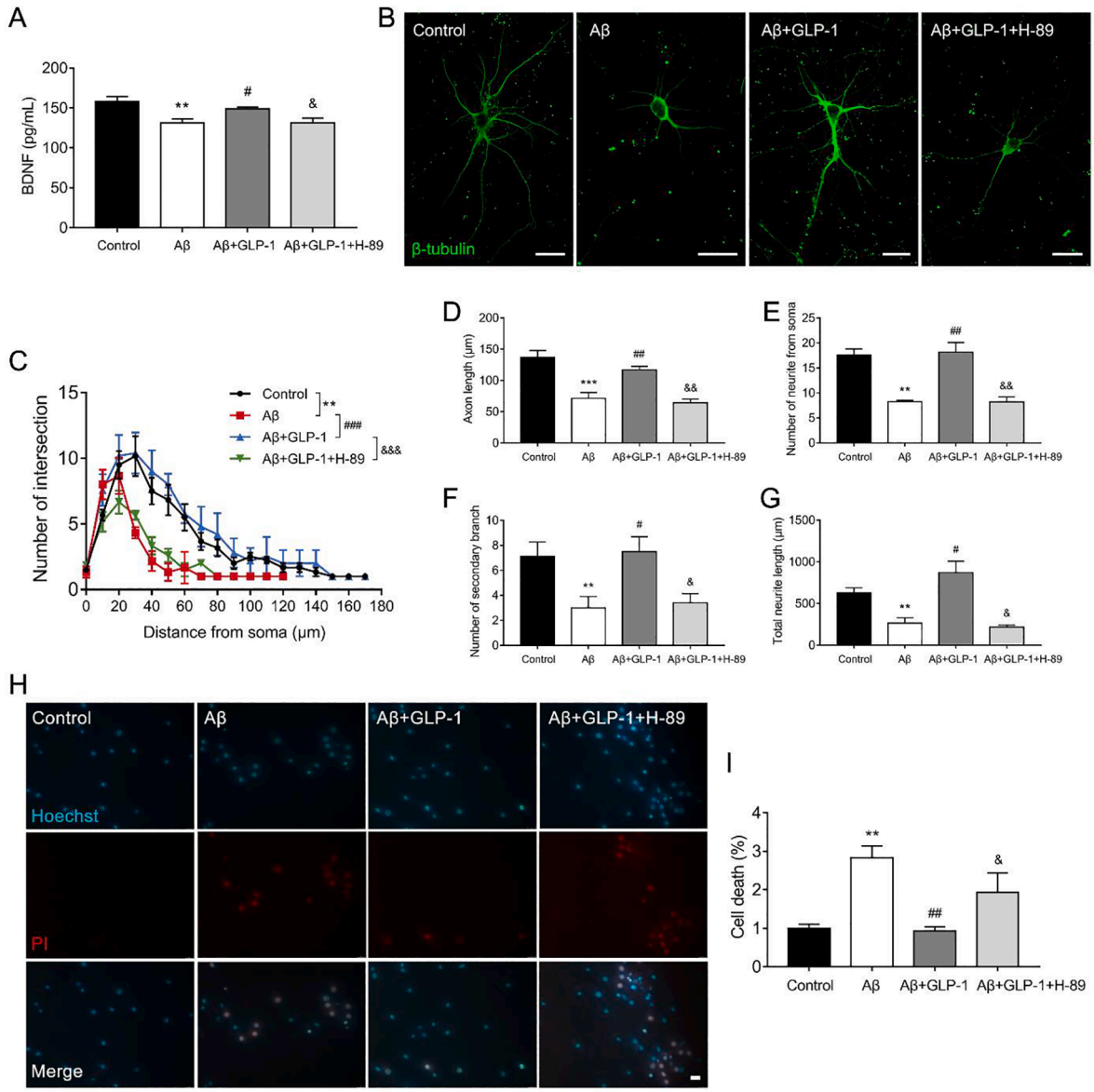

Fig. 4. GLP-1 improved the neuronal supportive ability of Aβ-treated astrocytes via the cAMP/PKA pathway. (A) BDNF secretion from astrocytes determined by ELISA. n = 5 wells/group. (B) Fluorescent images of neurons co-cultured with astrocytes immunostained against βIII-tubulin. Scale bar = 25 μm. (C) Neuronal complexity of neurons co-cultured with astrocytes determined by Sholl analysis. Axon length (D), number of neurite from soma (E), number of secondary branch (F), and total neurite length (G) were analyzed using the Image J software. n = 3 wells/group. (H) Hoechst and PI staining of neurons co-cultured with astrocytes. Scale bar = 10 μm. (I) Quantitative analysis of cell death (%). n = 3 wells/group. $^{**}P < 0.01$, $^{***}P < 0.001$ vs. Control; $\#P < 0.05$, $\#\#P < 0.01$ vs. Aβ; $\&P < 0.05$, $\&\&P < 0.01$ vs. Aβ + GLP-1.

and remodeling of mitochondrial cristae, where electron transport chain complexes are located, thus regulating mitochondrial respiration and ATP synthesis [50]. We also found that GLP-1 exerted beneficial effects on energy production and respiratory capacity in Aβ-treated astrocytes. Moreover, mitochondrial dysfunction drives ROS overproduction, resulting in cellular oxidative damage. Excessive ROS production contributes to collapsed MMP, followed by the opening of the mitochondrial permeability transition pore (MPTP), triggering cell death through the release of pro-apoptotic factors, such as cytochrome *c* [38,51]. Here, we revealed that GLP-1 improved the overproduction of mitochondrial ROS and restored the collapse of MMP, concomitantly protecting the viability of Aβ-treated astrocytes.

The mechanism of neuroprotection by GLP-1 is correlated with the activation of the cAMP/PKA pathway [52–54]. The cAMP/PKA pathway are involved in the regulation of mitochondrial fission and fusion [55,56]. PKA directly phosphorylates DRP1 at s637 and decreases its GTPase activity, resulting in inhibited mitochondrial fission [57]. cAMP locally activates PKA [58], leading to elongated mitochondria and increased MMP, and finally prevents apoptosis [59]. Aβ was reported to induce mitochondrial impairments in neuroblastoma cells, which were reversed following the activation of the cAMP-dependent PKA/CREB pathway [60]. Bao *et al.* reported that liraglutide exerted neuroprotective effects against AGE-induced oxidative stress, inflammation, and apoptosis in astrocytes via the GLP-1R-mediated activation of the cAMP/PKA/CREB pathway [61]. In our study, GLP-1 and its analogue elevated cAMP and PKA in both Aβ-treated astrocytes and 5 × FAD mice brain. We further demonstrated that inhibition of PKA by H-89 decreased p-DRP1 (s637) protein expression and induced mitochondrial fragmentation in Aβ + GLP-1 + H-89 group, subsequently reversing other beneficial effects of GLP-1 on Aβ-induced mitochondrial and cellular impairments in astrocytes. Thus, it could be speculated that GLP-1 decreases DRP1-mediated fission by activating the cAMP/PKA

pathway, thus improving mitochondrial dysfunction, and consequently promoting cell survival in astrocytes.

Previous studies reported that astrocytic dysfunction induced by mitochondrial abnormality aggravated neuron death in the perilesional area [62], and impaired cell survival of cultured neurons [11]. Our study demonstrated that mitochondrial malfunction of astrocytes resulted in impaired neuronal growth and survival, whereas GLP-1 improved the neuronal supportive ability of Aβ-treated astrocytes. Astrocytes secrete a variety of neurotrophic factors to protect neurons, such as BDNF [63,64]. However, astrocytic BDNF levels in 5 × FAD mice were significantly decreased in AD [65]. It has been suggested that Aβ in mitochondria attenuates BDNF-neurotrophic tyrosine receptor kinase 2 (TrkB) signaling and axon transport by impairing the mitochondrial dysfunction of neurons [42], implicating a correlation between mitochondrial function and neurotrophic function in AD. Pugazhenthi *et al.* reported that Aβ deposition downregulated BDNF expression via a cAMP-dependent pathway [66]. We found that in line with the suppression of the cAMP/PKA pathway, the secretion of BNDF was also decreased in Aβ-treated astrocytes, whereas GLP-1 upregulated the cAMP/PKA pathway, as well as the production of BDNF. Another study reported that GLP-1 could also upregulate BDNF expression in a PKA-dependent manner, subsequently inhibiting cell apoptosis in microglia [67]. The above findings might account for the effect of GLP-1 on preventing neuron loss in the brain of 5 × FAD mice, as shown in our results.

Collectively, we demonstrated that GLP-1 improved mitochondrial function, as well as neuronal supportive ability in astrocytes, and the mechanism underlying these effects was associated with the activation of the cAMP/PKA pathway, which was beneficial in preventing neuron loss in AD brain.

5. Conclusions

We demonstrated that GLP-1 exerts its neuroprotective effect in AD by improving mitochondrial function of astrocytes by activating the cAMP/PKA pathway. This study revealed a new mechanism behind the neuroprotective effect of GLP-1 in AD.

CRediT authorship contribution statement

Yunzhen Xie: Conceptualization, Writing - original draft. **Jiaping Zheng:** Writing - review & editing. **Shiqi Li:** Resources, Data curation. **Huiying Li:** Resources. **Yu Zhou:** Software. **Wenrong Zheng:** Resources. **Meilian Zhang:** Data curation. **Libin Liu:** Project administration. **Zhou Chen:** Supervision.

Declaration of Competing Interest

The authors declare that they have no known competing financial interests or personal relationships that could have appeared to influence the work reported in this paper.

Acknowledgments

This work was supported by Fujian Provincial Department of Finance, China (No. 2018B041), the Natural Science Foundation of Fujian Province, China (No. 2018J01841), the Science and Technology External Cooperation Program of Fujian Province, China (No. 2018I0007), and the Open Research Fund of Fujian Key Laboratory of Natural Medicine Pharmacology, Fujian Medical University, China (No. FJNMP-201901).

The authors would like to thank Ling Lin and Junjin Lin from the Public Technology Service Center (Fujian Medical University, Fuzhou, China) for their technical assistance.

References

[1] C. Acosta, H.D. Anderson, C.M. Anderson, Astrocyte dysfunction in Alzheimer disease, J. Neurosci. Res. 95 (12) (2017) 2430–2447.
[2] B.d. Pins, C. Cifuentes-Díaz, A.T. Farah, L. López-Molina, E. Montalban, A. Sancho-Balsells, et al., Conditional BDNF delivery from astrocytes rescues memory deficits, spine density, and synaptic properties in the 5xFAD mouse model of Alzheimer disease, J. Neurosci. 39 (13) (2019) 2441–2458.
[3] M. Olabarria, H.N. Noristani, A. Verkhratsky, J.J. Rodríguez, Concomitant astroglial atrophy and astrogliosis in a triple transgenic animal model of Alzheimer's disease, Glia 58 (7) (2010) 831–838.
[4] R.G. Nagele, M.R. D'Andrea, H. Lee, V. Venkataraman, H.-Y. Wang, Astrocytes accumulate A beta 42 and give rise to astrocytic amyloid plaques in Alzheimer disease brains, Brain Res. 971 (2) (2003) 197–209.
[5] E.T. Hsu, M. Gangolli, S. Su, L. Holleran, T.D. Stein, V.E. Alvarez, et al., Astrocytic degeneration in chronic traumatic encephalopathy, Acta Neuropathol. 136 (6) (2018) 955–972.
[6] J. Qiao, J. Wang, H. Wang, Y. Zhang, S. Zhu, A. Adilijiang, et al., Regulation of astrocyte pathology by fluoxetine prevents the deterioration of Alzheimer phenotypes in an APP/PS1 mouse model, Glia 64 (2) (2016) 240–254.
[7] S. Beggiato, T. Cassano, L. Ferraro, M.C. Tomasini, Astrocytic palmitoylethanolamide pre-exposure exerts neuroprotective effects in astrocyte-neuron co-cultures from a triple transgenic mouse model of Alzheimer's disease, Life Sci. 257 (2020), 118037.
[8] L.L. Dugan, J.-S. Kim-Han, Astrocyte mitochondria in vitro models of ischemia, J. Bioenerg. Biomembr. 36 (4) (2004) 317–321.
[9] E. Motori, Julien Puyal, Nicolas Toni, Alexander Ghanem, Cristina Angeloni, Marco Malaguti, et al., Inflammation-induced alteration of astrocyte mitochondrial dynamics requires autophagy for mitochondrial network maintenance, Cell Metab. 18 (6) (2013) 844–859.
[10] A.-R. Ko, H.-W. Hyun, S.-J. Min, J.-E. Kim, The differential DRP1 phosphorylation and mitochondrial dynamics in the regional specific astroglial death induced by status epilepticus, Front. Cell. Neurosci. 10 (2016) 124.
[11] J.G. Hoekstra, T.J. Cook, T. Stewart, H. Mattison, M.T. Dreisbach, Z.S. Hoffer, et al., Astrocytic dynamin-like protein 1 regulates neuronal protection against excitotoxicity in Parkinson disease, Am. J. Pathol. 185 (2) (2015) 536–549.
[12] Y. Liu, Y. Yan, Yasuyoshi Inagaki, Sarah Logan, Zeljko J Bosnjak, X. Bai, Insufficient astrocyte-derived brain-derived neurotrophic factor contributes to propofol-induced neuron death through Akt/Glycogen synthase kinase 3β/Mitochondrial Fission Pathway, Anesth. Analg. 125 (1) (2017) 241–254.
[13] Manuel van Gijsel-Bonnello, Kévin Baranger, Philippe Benech, Santiago Rivera, Michel Khrestchatisky, Max de Reggi, et al., Metabolic changes and inflammation in cultured astrocytes from the 5xFAD mouse model of Alzheimer's disease: Alleviation by pantethine, PLoS ONE 12 (4) (2017), e0175369.
[14] G. Dematteis, G. Vydmantaitė, F.A. Ruffinatti, M. Chahin, S. Farruggio, E. Barberis, et al., Proteomic analysis links alterations of bioenergetics, mitochondria-ER interactions and proteostasis in hippocampal astrocytes from 3xTg-AD mice, Cell Death Dis. 11 (8) (2020) 645.
[15] C. Hölscher, Potential role of glucagon-like peptide-1 (GLP-1) in neuroprotection, CNS drugs 26 (10) (2012) 871–882.
[16] T.D. Müller, B. Finan, S.R. Bloom, D. D'Alessio, D.J. Drucker, P.R. Flatt, et al., Glucagon-like peptide 1 (GLP-1), Mol. Metabol. 30 (2019) 72–130.
[17] P.L. McClean, V.A. Gault, P. Harriott, C. Hölscher, Glucagon-like peptide-1 analogues enhance synaptic plasticity in the brain: a link between diabetes and Alzheimer's disease, Eur. J. Pharmacol. 630 (1–3) (2010) 158–162.
[18] Y. Hou, S.A. Ernst, K. Heidenreich, J.A. Williams, Glucagon-like peptide-1 receptor is present in pancreatic acinar cells and regulates amylase secretion through cAMP, Am. J. Physiol. -Gastrointestinal Liver Physiol. 310 (1) (2016) G26–33.
[19] S.C. Cork, J.E. Richards, M.K. Holt, F.M. Gribble, F. Reimann, S. Trapp, Distribution and characterisation of Glucagon-like peptide-1 receptor expressing cells in the mouse brain, Mol. Metabol. 4 (10) (2015) 718–731.
[20] R. Göke, P.J. Larsen, J.D. Mikkelsen, S.P. Sheikh, Distribution of GLP-1 binding sites in the rat brain: evidence that exendin-4 is a ligand of brain GLP-1 binding sites, Eur. J. Neurosci. 7 (11) (1995) 2294–2300.
[21] C. Hölscher, The role of GLP-1 in neuronal activity and neurodegeneration, Vitam. Horm. 84 (2010) 331–354.
[22] Z. Yu, T. Jin, New insights into the role of cAMP in the production and function of the incretin hormone glucagon-like peptide-1 (GLP-1), Cell. Signal. 22 (1) (2010) 1–8.
[23] V. Calsolaro, P. Edison, Novel GLP-1 (Glucagon-Like Peptide-1) Analogues and Insulin in the Treatment for Alzheimer's Disease and Other Neurodegenerative Diseases, CNS Drugs 29 (12) (2015) 1023–1039.
[24] T. Ma, X. Du, J.E. Pick, G. Sui, M. Brownlee, E. Klann, Glucagon-like peptide-1 cleavage product GLP-1(9–36) amide rescues synaptic plasticity and memory deficits in Alzheimer's disease model mice, J. Neurosci. 32 (40) (2012) 13701–13708.
[25] P.L. McClean, C. Hölscher, Liraglutide can reverse memory impairment, synaptic loss and reduce plaque load in aged APP/PS1 mice, a model of Alzheimer's disease, Neuropharmacology 76 (Pt A) (2014) 57–67.
[26] Liqin Qi, Zhou Chen, Yanping Wang, Xiaoying Liu, Xiaohong Liu, Linfang Ke, et al., Subcutaneous liraglutide ameliorates methylglyoxal-induced Alzheimer-like tau pathology and cognitive impairment by modulating tau hyperphosphorylation and glycogen synthase kinase-3β, Am. J. Transl. Res. 9 (2) (2017) 247–260.
[27] J. An, Y. Zhou, M. Zhang, Y. Xie, S. Ke, L. Liu, et al., Exenatide alleviates mitochondrial dysfunction and cognitive impairment in the 5×FAD mouse model of Alzheimer's disease, Behav. Brain Res. 370 (2019), 111932.

[28] H. Oakley, S.L. Cole, S. Logan, E. Maus, P. Shao, J. Craft, et al., Intraneuronal beta-amyloid aggregates, neurodegeneration, and neuron loss in transgenic mice with five familial Alzheimer's disease mutations: potential factors in amyloid plaque formation, J. Neurosci. 26 (40) (2006) 10129–10140.
[29] E.B. Westcott, S.S. Segal, Ageing alters perivascular nerve function of mouse mesenteric arteries in vivo, J. Physiol. -London 591 (5) (2013) 1251–1263.
[30] M.A. Kuszczyk, Sandrine Sanchez, Joanna Pankiewicz, Jungsu Kim, Malgorzata Duszczyk, Maitea Guridi, et al., Blocking the interaction between apolipoprotein E and Aβ reduces intraneuronal accumulation of Aβ and inhibits synaptic degeneration, Am. J. Pathol. 182 (5) (2013) 1750–1768.
[31] G. Yoon, Y.-K. Kim, J. Song, Glucagon-like peptide-1 suppresses neuroinflammation and improves neural structure, Pharmacol. Res. 152 (2020), 104615.
[32] F.M. An, S. Chen, Z. Xu, L. Yin, Y. Wang, A.R. Liu, et al., Glucagon-like peptide-1 regulates mitochondrial biogenesis and tau phosphorylation against advanced glycation end product-induced neuronal insult: Studies in vivo and in vitro, Neuroscience 300 (2015) 75–84.
[33] C.J. Garwood, A.M. Pooler, J. Atherton, D.P. Hanger, W. Noble, Astrocytes are important mediators of Aβ-induced neurotoxicity and tau phosphorylation in primary culture, Cell Death Dis. 2 (6) (2011), e167.
[34] C.H. Serezani, M.N. Ballinger, D.M. Aronoff, M. Peters-Golden, Cyclic AMP: master regulator of innate immune cell function, Am. J. Respir. Cell Mol. Biol. 39 (2) (2008) 127–132.
[35] S.Y. Lee, H.J. Kim, Woo Jong Lee, S.H. Joo, S.-J. Jeon, J.W. Kim, et al., Differential regulation of matrix metalloproteinase-9 and tissue plasminogen activator activity by the cyclic-AMP system in lipopolysaccharide-stimulated rat primary astrocytes, Neurochem. Res. 33 (11) (2008) 2324–2334.
[36] J.S. Bhatti, G.K. Bhatti, P.H. Reddy, Mitochondrial dysfunction and oxidative stress in metabolic disorders - a step towards mitochondria based therapeutic strategies, Biochim. Biophys. Acta – Mol. Basis Dis. 1863 (5) (2017) 1066–1077.
[37] H. Li, A. Ham, T.C. Ma, S.H. Kuo, E. Kanter, D. Kim, et al., Mitochondrial dysfunction and mitophagy defect triggered by heterozygous GBA mutations, Autophagy 15 (1) (2019) 113–130.
[38] N. Tajeddine, How do reactive oxygen species and calcium trigger mitochondrial membrane permeabilisation? Biochim. Biophys. Acta 1860 (6) (2016) 1079–1088.
[39] P. Mishra, D.C. Chan, Metabolic regulation of mitochondrial dynamics, J. Cell Biol. 212 (4) (2016) 379–387.
[40] G. Twig, O.S. Shirihai, The interplay between mitochondrial dynamics and mitophagy, Antioxid. Redox Signal. 14 (10) (2011) 1939–1951.
[41] X. Zhu, George Perry, Mark A Smith, X. Wang, Abnormal mitochondrial dynamics in the pathogenesis of Alzheimer's disease, J. Alzheimers Dis. 33 (Suppl 1(0 1)) (2013) S253–262.
[42] X. Ye, W. Tai, D. Zhang, The early events of Alzheimer's disease pathology: from mitochondrial dysfunction to BDNF axonal transport deficits, Neurobiol. Aging 33 (6) (2012), 1122.e1121 1110.
[43] H.M. Wilkins, R.H. Swerdlow, Amyloid precursor protein processing and bioenergetics, Brain Res. Bull. 133 (2017) 71–79.
[44] Pallabi Sarkar, Ivan Zaja, Martin Bienengraeber, Kevin R. Rarick, Maia Terashvili, Scott Canfield, et al., Epoxyeicosatrienoic acids pretreatment improves amyloid β-induced mitochondrial dysfunction in cultured rat hippocampal astrocytes, Am. J. Physiol. Heart Circul. Physiol. 306 (4) (2014) H475–484.
[45] A.Y. Abramov, L. Canevari, M.R. Duchen, Beta-amyloid peptides induce mitochondrial dysfunction and oxidative stress in astrocytes and death of neurons through activation of NADPH oxidase, J. Neurosci. 24 (2) (2004) 565–575.
[46] María Dolores Martin-de-Saavedra, Elisa Navarro, Ana J. Moreno-Ortega, Mauricio P. Cunha, Izaskun Buendia, Pablo Hernansanz-Agustín, et al., The APPswe/PS1A246E mutations in an astrocytic cell line leads to increased vulnerability to oxygen and glucose deprivation, Ca dysregulation, and mitochondrial abnormalities, J. Neurochem. 145 (2) (2018) 170–182.
[47] S. Jantrapirom, W. Nimlamool, N. Chattipakorn, S. Chattipakorn, P. Temviriyanukul, W. Inthachat, et al., Liraglutide Suppresses Tau Hyperphosphorylation, Amyloid Beta Accumulation through Regulating Neuronal Insulin Signaling and BACE-1 Activity, Int. J. Mol. Sci. 21 (5) (2020).
[48] T. Perry, D.K. Lahiri, K. Sambamurti, D. Chen, M.P. Mattson, J.M. Egan, et al., Glucagon-like peptide-1 decreases endogenous amyloid-beta peptide (Abeta) levels and protects hippocampal neurons from death induced by Abeta and iron, J. Neurosci. Res. 72 (5) (2003) 603–612.
[49] D. Garabadu, J. Verma, Exendin-4 attenuates brain mitochondrial toxicity through PI3K/Akt-dependent pathway in amyloid beta (1–42)-induced cognitive deficit rats, Neurochem. Int. 128 (2019) 39–49.
[50] N. Baker, J. Patel, M. Khacho, Linking mitochondrial dynamics, cristae remodeling and supercomplex formation: How mitochondrial structure can regulate bioenergetics, Mitochondrion 49 (2019) 259–268.
[51] D.R. Green, G. Kroemer, The pathophysiology of mitochondrial cell death, Science 305 (5684) (2004) 626–629.
[52] A.F. Batista, L. Forny-Germano, J.R. Clarke, E.S.N.M. Lyra, J. Brito-Moreira, S. E. Boehnke, et al., The diabetes drug liraglutide reverses cognitive impairment in mice and attenuates insulin receptor and synaptic pathology in a non-human primate model of Alzheimer's disease, J. Pathol. 245 (1) (2018) 85–100.
[53] Y. Li, M. Bader, I. Tamargo, V. Rubovitch, D. Tweedie, C.G. Pick, et al., Liraglutide is neurotrophic and neuroprotective in neuronal cultures and mitigates mild traumatic brain injury in mice, J. Neurochem. 135 (6) (2015) 1203–1217.
[54] E. Candeias, I. Sebastião, S. Cardoso, C. Carvalho, M.S. Santos, C.R. Oliveira, et al., Brain GLP-1/IGF-1 signaling and autophagy mediate exendin-4 protection against apoptosis in type 2 diabetic rats, Mol. Neurobiol. 55 (5) (2018) 4030–4050.
[55] W. Ml, C. Wh, L. Ih, T. Cd, W. Sm, A novel effect of cyclic AMP on capacitative Ca^{2+} entry in cultured rat cerebellar astrocytes, J. Neurochem. 73 (3) (1999) 1318–1328.
[56] Y.O. Amer, E. Hebert-Chatelain, Mitochondrial cAMP-PKA signaling: what do we really know? Biochim. Biophys. Acta - Bioenergetics 1859 (9) (2018) 868–877.
[57] C.-R. Chang, C. Blackstone, Cyclic AMP-dependent protein kinase phosphorylation of Drp1 regulates its GTPase activity and mitochondrial morphology, J. Biol. Chem. 282 (30) (2007) 21583–21587.
[58] W.-K. Ju, M.S. Shim, K.-Y. Kim, T.L. Park, S. Ahn, G. Edwards, et al., Inhibition of cAMP/PKA pathway protects optic nerve head astrocytes against oxidative stress by Akt/Bax phosphorylation-mediated Mfn1/2 oligomerization, Oxid. Med. Cell. Longevity 2019 (2019) 8060962.
[59] Stefania Monterisi, Miguel J. Lobo, Craig Livie, John C. Castle, Michael Weinberger, George Baillie, et al., PDE2A2 regulates mitochondria morphology and apoptotic cell death via local modulation of cAMP/PKA signalling, eLife 6 (2017), e21374.
[60] B. Sheng, X. Wang, B. Su, H.G. Lee, G. Casadesus, G. Perry, et al., Impaired mitochondrial biogenesis contributes to mitochondrial dysfunction in Alzheimer's disease, J. Neurochem. 120 (3) (2012) 419–429.
[61] Y. Bao, L. Jiang, H. Chen, J. Zou, Z. Liu, Y. Shi, The neuroprotective effect of liraglutide is mediated by glucagon-like peptide 1 receptor-mediated activation of cAMP/PKA/CREB pathway, Cell. Physiol. Biochem. 36 (6) (2015) 2366–2378.
[62] C. Fiebig, S. Keiner, B. Ebert, I. Schäffner, R. Jagasia, D.C. Lie, et al., Mitochondrial dysfunction in astrocytes impairs the generation of reactive astrocytes and enhances neuronal cell death in the cortex upon photothrombotic lesion, Front. Mol. Neurosci. 12 (2019) 40.
[63] R. Cabezas, E. Baez-Jurado, O. Hidalgo-Lanussa, V. Echeverria, G.M. Ashrad, A. Sahebkar, et al., Growth factors and neuroglobin in astrocyte protection against neurodegeneration and oxidative stress, Mol. Neurobiol. 56 (4) (2019) 2339–2351.
[64] M. Orre, W. Kamphuis, L.M. Osborn, A.H.P. Jansen, L. Kooijman, K. Bossers, et al., Isolation of glia from Alzheimer's mice reveals inflammation and dysfunction, Neurobiol. Aging 35 (12) (2014) 2746–2760.
[65] I. Belaya, M. Ivanova, A. Sorvari, M. Ilicic, S. Loppi, H. Koivisto, et al., Astrocyte remodeling in the beneficial effects of long-term voluntary exercise in Alzheimer's disease, J. Neuroinflammation 17 (1) (2020) 271.
[66] Y. Xu, N. Zhu, W. Xu, H. Ye, K. Liu, F. Wu, et al., Inhibition of phosphodiesterase-4 reverses Aβ-induced memory impairment by regulation of HPA axis related cAMP signaling, Front. Aging Neurosci. 10 (2018) 204.
[67] L.J. Spielman, D.L. Gibson, A. Klegeris, Incretin hormones regulate microglia oxidative stress, survival and expression of trophic factors, Eur. J. Cell Biol. 96 (3) (2017) 240–253.